Available online at www.sciencedirect.com
SCIENCE DIRECT®
Bioorganic & Medicinal Chemistry Letters 14 (2004) 2817–2822
Bioorganic & Medicinal Chemistry Letters

Hit-to-lead studies: the discovery of potent, orally active, thiophenecarboxamide IKK-2 inhibitors

Andrew Baxter,[a,*] Steve Brough,[a] Anne Cooper,[a] Eike Floettmann,[a] Steve Foster,[b] Christine Harding,[b] Jason Kettle,[b] Tom McInally,[a] Craig Martin,[a] Michelle Mobbs,[b] Maurice Needham,[b] Pete Newham,[b] Stuart Paine,[a] Steve St-Gallay,[a] Sylvia Salter,[a] John Unitt[a] and Yafeng Xue[c]

[a]*AstraZeneca R&D Charnwood, Bakewell Road, Loughborough LE11 5RH, UK*
[b]*AstraZeneca R&D Alderley Park, Cheshire, Macclesfield SK10 4TG, UK*
[c]*Structural Chemistry Laboratory, AstraZeneca R&D Mölndal, S-431 83 Mölndal, Sweden*

Received 12 December 2003; revised 5 March 2004; accepted 19 March 2004

Abstract—A hit-to-lead optimisation programme was carried out on the thiophenecarboxamide high throughput screening hits **1** and **2** resulting in the discovery of the potent and orally bioavailable IKK-2 inhibitor **22**.

The use of high throughput screening (HTS) is now widespread in the pharmaceutical industry. There was an expectation that once a screen was established for a particular target then potent lead compounds or candidate drugs would be found. The reality is often far from this. Bridging the gap between the end of a HTS and the start of a full lead optimisation (LO) project has been described as hit-to-lead (HtL).[1] Hits from HTS are profiled and compared to generic lead criteria. The lead target profile used is shown in Figure 1. Lead series then have a balance of properties—potency, SAR and an encouraging metabolic and selectivity profile—such that rapid lead optimisation should provide a candidate drug (CD) in less than 2 years.

Nuclear factor κB (NF-κB) transcription factors are composed of homo- and heterodimers of the *Rel* family of DNA-binding proteins.[2] A key role of these transcription factors is to induce and coordinate the expression of a broad spectrum of pro-inflammatory genes including cytokines, chemokines, interferons, MHC proteins, growth factors and cell adhesion molecules.[3] NF-κB is normally retained in the cytoplasm by IκB, however, upon cellular activation, IκB is phosphorylated by an IκB kinase (IKK) and is subsequently degraded. Free NF-κB then translocates to the nucleus where it mediates proinflammatory gene expression. There are three classical IκB's: IκBα, IκBβ and IκBε; all require the phosphorylation of two key serine residues

Potency	$IC_{50} < 0.1\mu M$
Rat Hepatocytes	clearance < 14μL/min/10^6 cells
Human Liver Microsomes	clearance < 23μL/min/mg
Rat iv PK	clearance < 35mL/min/kg, Vss > 0.5L/kg, $T_{1/2} > 0.5$hr
Oral Bioavailability	F > 10%, PPB < 99.5%
Physical Chemical	MWt < 450, clogP < 3.0, logD < 3.0
Additionally: Clear SAR, Appropriate selectivity data and Patentable.	

Figure 1. Hit-to-lead generic lead target profile.

Keywords: Hit-to-lead; IKK inhibitor; Kinase.
* Corresponding author. Tel.: +44-(0)1509-644772; fax: +44-(0)1509-645513; e-mail: andrew.jg.baxter@astrazeneca.com

0960-894X/$ - see front matter
doi:10.1016/j.bmcl.2004.03.058

before they can be degraded. Two major enzymes appear to be responsible for IκB phosphorylation: IKK-1 and IKK-2.[4] Dominant-negative (DN) versions of either IKK-1 or IKK-2 (where ATP binding is disabled by the mutation of a key kinase domain residue) were found to suppress the activation of NF-κB by TNF-α, IL-1β, LPS and CD3/CD28 crosslinking; importantly IKK-2 DN was found to be a far more potent inhibitor than IKK-1 DN.[5–7] Furthermore, the generation of IKK-1 and IKK-2 deficient mice has established the requirement of IKK-2 for activation of NF-κB by proinflammatory stimuli and reinforced the dominant role of IKK-2 suggested by biochemical data. Indeed it was demonstrated that IKK-1 was dispensable for NF-κB activation by these stimuli.[8–10] Thus, inhibition of IKK-2 represents a potentially attractive target for modulation of immune function and hence the development of drugs for the treatment of auto-immune diseases.

As part of an IKK-2 inhibitor program, the AZ compound collection was screened in a scintillation proximity assay (SPA) kinase assay that employed recombinant IKK-2 and a GST-IκBα fusion protein. The activity and potency of hits were confirmed using 'filter wash' kinase assays for both IKK-2 and IKK-1.[11,12] Whole cell activity was determined using the inhibition of LPS TNF-α production in peripheral blood mononuclear cells (PBMCs).[11,13] Cell toxicity was also measured in PBMCs using a WST-1 assay.[13]

The profiles of the thiophenecarboxamides **1**[14] and **2** are shown in Table 1, compared with the key lead criteria—potency against isolated enzyme and in cells, in vitro metabolic clearance by rat hepatocytes and human liver microsomes, molecular weight and lipophilicity. The amides have reasonable potency especially for their low molecular weights, and metabolic stability is acceptable at this stage. Comparison of the structures of the two hits **1** and **2** prompted the synthesis of **3**. This compound (**3**) was found to have an excellent combination of potency, low molecular weight and log *D*. The 3-thienyl group was potentially metabolically labile and so was replaced by a phenyl group (compound **4**) with no loss of potency and improved in vitro metabolic stability. Compound **4** is in fact close to the lead criteria and also possesses good TNF inhibitory activity. The focus of the present study then became the remaining issues of solubility, mediocre metabolic stability and understanding of SAR with particular reference to the likely binding mode.

The compounds were synthesised by the routes shown in Scheme 1. The parent aminothiophenecarboxylates were prepared by cyclisation of methyl mercaptoacetate with aroylacrylonitriles that were in turn prepared from the corresponding acetophenones.[15] Ester hydrolysis gave the aminoacids, which were converted to the aminoamides via thionyl chloride treatment followed by reaction with the appropriate amine or ammonia (compound **5**). The aminoamides were reacted with either trimethylsilylisocyanate or sodium isocyanate in aqueous acetic acid to give the unsubstituted ureas **3**, **4**, **16**–**22**. Reaction of the aminoamide with alkylisocyanates gave the substituted ureas **8** and **9**. Alternatively the aminoacid could be converted by phosgene to the oxazinedione, which reacted with amines to give the ureidoacids. Thionyl chloride treatment followed by reaction with ammonia gave the substituted ureas **10** and **11**. The isomeric thiophene **13**, imidazole **14** and pyrazine **15** were prepared from the corresponding documented amino heterocycles.

Using the carboxamide **4** as a starting point, an exploration of SAR was undertaken focusing in turn on the amide and urea, central thiophene ring and phenyl substitution. Table 2 details the effects of simple substitution on the urea and amide nitrogens. First it should be noted that the potency increase observed for the amine to urea transformation is almost identical for the 3-thienyl (**1** to **3**) and phenyl (**5** to **4**). Mono and dimethylation of the amide caused complete loss of activity (**4** vs **6** and **7**). Mono-methylation of the terminal urea nitrogen caused some loss of potency (**8** vs **4**) but larger groups (ethyl **9** or benzyl **10**) and dimethylation (**11**) ablated all activity. Parallel synthesis of a range of amides (i.e., R3 = COR) also gave only inactive compounds (data not shown). Sulfonamides (e.g., **12**) had weak activity. The SAR of the amide and urea indicates that all of the H-bond donors and acceptors are either required for active site kinase interactions or that sub-

Table 1. Profile of thiophenes **1** to **4**

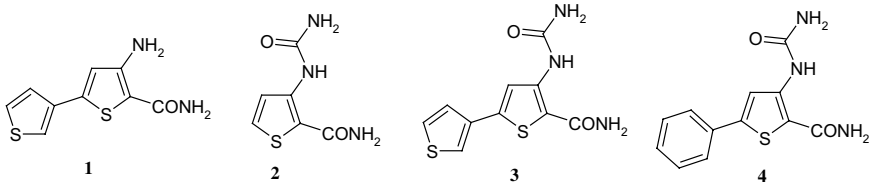

Generic lead criteria	1	2	3	4
IKK-2 enzyme $IC_{50} < 0.1\,\mu M$	1.6	2.0	0.063	0.025
PBMC TNF inhib $IC_{50} < 0.3\,\mu M$	6.3	>10	0.50	0.25
Rat hepatocyte clearance $<14\,\mu L/min/10^6$ cells	18	14	21	3
Human microsome clearance $<23\,\mu L/min/mg$	30	49	43	27
Molecular weight <450	224	185	267	261
log *D* < 3.0	2.2	0.04	1.7	2.4

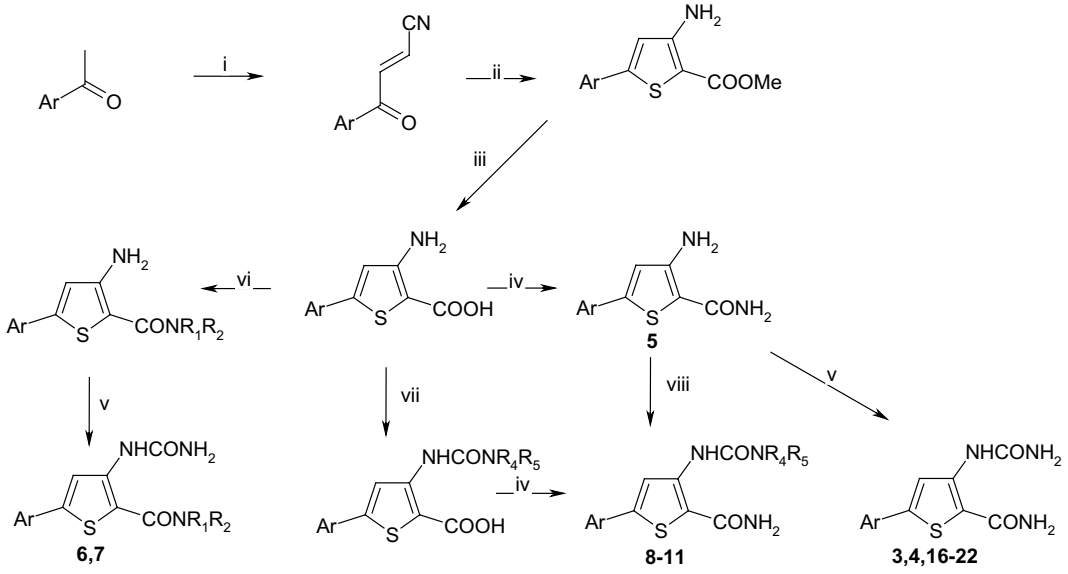

Scheme 1. (i) $POCl_3$, DMF then $NH_2OH{\cdot}HCl$; (ii) $HACH_2CO_2Me$, NaOH, MeOH; (iii) NaOH, aq MeOH; (iv) $SOCl_2$ then NH_3, CH_3CN; (v) TMSNCO, DMF, CH_2Cl_2 or NaOCN, aq AcOH; (vi) $SOCl_2$ then $R_1R_2NH_2$; (vii) $COCl_2$ then R_4R_5NH; (viii) R_4NCO, toluene.

Table 2. IKK-2 inhibitory potencies—amide and urea variation

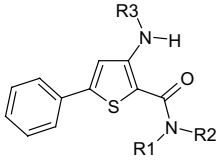

	R1	R2	R3	IKK-2 IC_{50} (μM)[a]
4	H	H	$CONH_2$	0.025
5	H	H	H	3.2
6	Me	H	$CONH_2$	NA
7	Me	Me	$CONH_2$	NA
8	H	H	CONHMe	0.05
9[b]	H	H	CONHEt	NA
10	H	H	$CONHCH_2Ph$	NA
11	H	H	$CONMe_2$	NA
12	H	H	SO_2(4-FPh)	1.6

[a] NA = <50% inhibition at 10 μM.
[b] 4-Fluorophenyl.

Table 3. IKK-2 inhibitory potencies—central thiophene variation

		IKK-2 IC_{50} (μM)
4	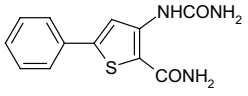	0.025
13	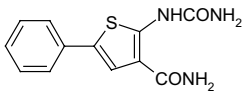	0.013
14	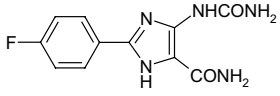	2.0
15	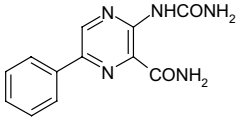	10

stitution causes disruption of the optimum binding orientation. Some confirmation of this hypothesis was obtained from modelling studies and from an X-ray crystal structure of a carboxamide inhibitor bound in a related kinase (see below).

Only limited variation of the central thiophene core was undertaken at this stage (Table 3). Interestingly the isomeric thiophene (**13**) retained all activity whilst the imidazole (**14**) and pyrazine (**15**) had much reduced potency. As stated previously, the orientation of the urea and amide would be expected to be important and it may be that internal hydrogen bonds between the urea NH and heterocyclic ring nitrogens prevent this active arrangement in the imidazole **14** and pyrazine **15**.

The focus of this study now shifted to explore variation of the phenyl substituent on amide **4** and its effect on a wider range of parameters. Table 4 has data on IKK-2 versus IKK-1 selectivity, TNF inhibition in cells versus cell toxicity and primary in vitro DMPK data. The profile of the unsubstituted phenyl compound **4** shows good IKK-2 potency with 40-fold selectivity versus IKK-1 together with good cellular activity associated with very weak cell toxicity. Variation of the phenyl substituents has only a modest effect on potency, selectivity or cell activity. Addition of electron withdrawing substituents in the 2, 3 or 4 position led to compounds that were all equiactive (**4** vs **19**, **20** and **22**). A slight fall in enzyme potency was seen with electron donating substituents (**4** vs **16**–**18** and **21**). This variation was only

Table 4. IKK-2 inhibitory potencies—phenyl variation

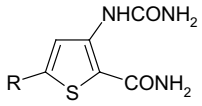

	R	IKK-2 IC_{50} (μM)	IKK-1 IC_{50} (μM)	TNF cell IC_{50} (μM)	WST tox IC_{50} (μM)	Rat heps[a]	Hu mics[a]	Sol (μg/mL)
2	H	2.0	NA	NA	NA	14	49	>50
3	3-Thienyl	0.063	5.0	0.5	NA	21	43	34
4	Ph	0.025	1.0	0.25	10	3	27	6
16	2-MeOPh	0.20	10	0.79	NA	17	16	23
17	3-MeOPh	0.30	7.9			13	44	
18	4-MeOPh	0.05	5.0	0.25	NA	10	54	2
19	2-ClPh	0.1	6.3			21	1	5
20	3-ClPh	0.04	2.5	0.16	NA	24	10	
21	3-HOPh	0.1	3.2	0.50	NA			45
22	4-FPh	0.063	6.3	0.40	NA	2	8	1.2

[a] Units as in Figure 1.

small and disappeared in the whole cell assays—compounds **3**, **4**, **10**, **18** and **20**–**22** all being essentially equiactive as inhibitors of TNF production. This level of cell activity was normally not associated with any cell toxicity.

A key component of the hit-to-lead process is to provide lead compounds with acceptable DMPK. To this end the more potent inhibitors in Table 4 were profiled in rat hepatocytes and human liver microsome preparations. Clearance of the parent thiophene **3** just exceeded the lead criteria limits and the phenyl compound **4** was borderline in human microsomes but stable in rat hepatocytes. Other analogues though were found to give improvements probably due to prevention of the predicted oxidative aryl metabolism. Substitution by simple electron donating substituents caused increased metabolic clearance consistent with increased susceptibility to oxidative attack on the electron rich phenyl rings (**4** vs **3** and **16**–**18**). The expected clearance reductions were observed, at least for the human microsomes, by the addition of electron withdrawing substituents (**4** vs **19**, **20** and especially **22**). Selected compounds in this study were tested in vivo for pharmacokinetic properties (Table 5). An initial in vitro assessment of the bioavailability potential was undertaken using Caco2 permeability. Results obtained in vivo subsequently confirmed the in vitro data. The thiophene **3** was rapidly cleared and the phenyl and fluorophenyl analogues (**4** and **22**) had lower clearance and were orally bioavailable, consistent with in vitro rat hepatocyte and Caco2 data.

A crystal structure of IKK-2 was not available, so a model of the protein was constructed. A sequence alignment was performed for all the kinase structures available from the Brookhaven Database at the time of the study, along with several AZ proprietary kinase structures and human IKK-2[16] (accession code 080158). Four template structures were selected: Brookhaven code 1AQ1[17] (a cell division protein kinase at 2.2 Å resolution); Brookhaven code 1HCK[18] (a cell division protein kinase at 1.9 Å resolution); Brookhaven code 1AD5[19] (a protein tyrosine kinase at 2.6 Å resolution) and 2HCK[19] (a protein tyrosine kinase at 3.0 Å resolution). These were used to generate 10 models of human IKK-2 using MODELLER v5.0,[20] and the model with the lowest objective function was selected. All hydrogen atoms were then added to this model using CHARMm[21] v25.2 with parameters v22. Automated docking programs did not place the compounds at the ATP binding site without pre-specifying the binding mode with constraints. This is possibly due to the closed nature of the pocket and the known conformational flexibility of kinases that can open out and then close around a ligand. It was decided to model the compounds in the

Table 5. DMPK parameters, Caco2 and plasma protein binding

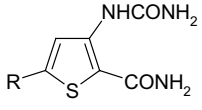

	R	Rat heps[a]	Caco2	In vivo rat pharmacokinetics[a]				PPB (%)
				Cl	Vss	T1/2	F	
3	3-Thienyl	21	10.2	51	1.6	0.4	7	93.1
4	Ph	3	17.7	18	3.2	2.5	27	94.9
22	4-FPh	2	12.2	6	0.7	1.4	78	92.5

[a] Units as in Figure 1.

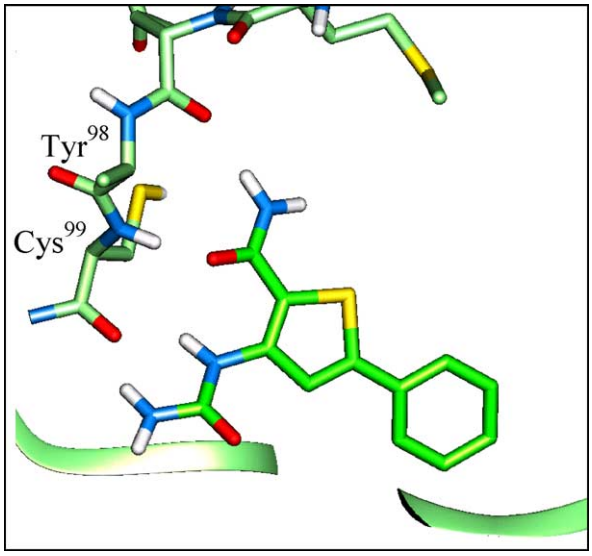

Figure 2. Human IKK-2 model complexed with compound **4**, showing the key hydrogen bond network.

active site manually, using the available compound SAR and knowledge of inhibitor binding to other kinases to determine the initial binding mode. An energy minimisation was performed using CHARMm for the protein ligand complex with some restraints. The result for compound **4** is shown in Figure 2.

It was possible to obtain structural data from the related kinase, JNK-1. Even though the sequence identity for the kinase domains of human JNK-1 and human IKK-2 is only 16%, compound **4** has a JNK-1 IC_{50} of 1.6 μM and the structure of this compound complexed with human JNK-1 was obtained at 2.1 Å resolution. Overlaying the two kinase domains by the Cα atoms that are similar between the protein sequences confirms the modelled IKK-2 binding mode, with all the predicted hydrogen bonds appearing in the X-ray structure (see Fig. 3). There is some discrepancy since the loop around

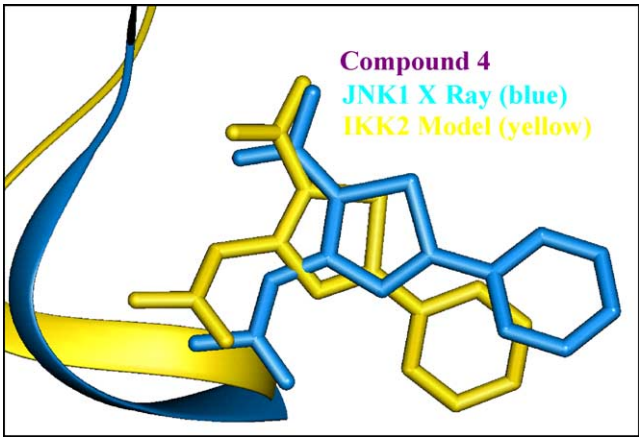

Figure 3. Overlay of the X-ray structure of compound **4** complexed with human JNK-1 (blue) with the model of compound **4** IKK-2 complex (yellow).

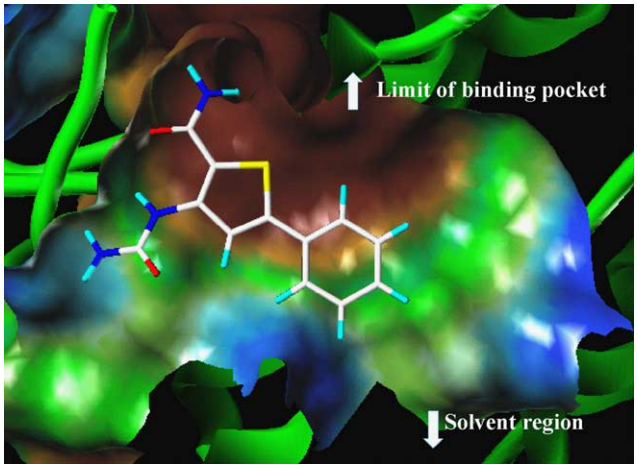

Figure 4. IKK-2 model complexed with compound **4** showing the Connolly solvent accessible surface coloured by lipophilicity. Brown represents more lipophilic regions, blue show more hydrophilic regions.

Cys99 in IKK-2 model is different from JNK-1 in the same region due to nonhomologous sequences.

Figure 4 shows the IKK-2 model complexed with compound **4** highlighting the Connolly solvent accessible[22] surface coloured by lipophilicity.[23] Brown represents more lipophilic regions, blue show more hydrophilic regions. This model helps to explain some of the SAR seen in Tables 2 and 4. From Table 2, substitution on the amide nitrogen (R1 and R2) disrupts the hydrogen bond with the backbone carbonyl of residue Tyr98, but also the space in this region is tight, so it is not surprising that compounds **6** and **7** are inactive. Substitution off the urea group (R3) will put groups out into a solvent accessible region, so the lipophilic substitutions in compounds **8**, **9** and **10** are less active. Removal of the hydrogen bond and replacement with a methyl group also produced an inactive compound (compound **11**) that can be explained by the model in terms of steric clash and loss of a key hydrogen bond. Table 4 shows how a variety of lipophilic thiophene substitutions are tolerated. This region is structurally rather featureless in the plane of the aromatic ring, but there is little space above and below the plane of the ring. The pocket is generally quite lipophilic, becoming less so as the solvent region is approached. This explains why a variety of hydrophobic substitutions that maintain the flatness of the molecule are well tolerated.

Combination of the structural features present in the HTS hits **1** and **2** led to the potent inhibitor **3**. Alteration of the metabolically labile thiophene to phenyl and then to the more stable 4-fluorophenyl led to the identification of the thiophenecarboxamide **22** as a potent, orally active IKK-2 inhibitor that fulfilled almost all of the lead criteria shown in Fig. 1. Poor solubility was the only continuing deficiency that was progressed as a potential problem for a future lead optimisation programme. The poor solubility though did not affect the oral bioavailability of this compound. The series was accepted as the basis for a new IKK-2 lead optimisation project.

References and notes

1. Michne, W. F. *Pharm. News* **1996**, *3*, 19.
2. Baldwin, A. S. *Annu. Rev. Immunol.* **1996**, *14*, 649.
3. Pahl, H. L. *Oncogene* **1999**, *18*, 6853.
4. Perkins, N. D. *Trends Biochem. Sci.* **2000**, *9*, 434.
5. Zandi, E.; Rothwarf, D. M.; Delhasse, M.; Hayakawa, M.; Karin, M. *Cell* **1997**, *91*, 243.
6. Mercurio, F.; Zhu, H.; Murray, B. W.; Shevchenko, A.; Bennett, B. L.; Li, J.; Young, B. D.; Barbosa, M.; Mann, M.; Manning, A.; Rao, A. *Science* **1997**, *278*, 860.
7. Woronicz, J. D.; Gao, X.; Cao, Z.; Rothe, M.; Goeddel, D. V. *Science* **1997**, *278*, 866.
8. Tanaka, M.; Fuentes, M. E.; Yamaguchi, K.; Durnin, M. H.; Dalrymple, S. A.; Hardy, K. L.; Goeddel, D. V. *Immunity* **1999**, *10*, 421.
9. Li, Q.; Van Antwerp, D.; Mercurio, F.; Lee, K. F.; Verma, I. M. *Science* **1999**, *284*, 321.
10. Li, Z. W.; Chu, W.; Hu, Y.; Delhase, M.; Deerinck, T.; Ellisman, M.; Johnson, R.; Karin, M. *J. Exp. Med.* **1999**, *189*, 1839.
11. For full details of the biological assays used see: Baxter, A.; Brough, S.; Faull, A.; Johnstone, C.; McInally, T. Int. Patent Appl. WO 01/58890.
12. Recombinant IKK enzymes and GST-IκBα were prepared as described.[11] IKK-2 kinase activity was determined using a 'filter kinase assay'. A GST-IκBα (1–53) fusion protein was used as a substrate for IKK-1 and IKK-2. Briefly, 96-well plates containing 50 μL reactions of 150 ng IKK-2 and 540 ng GST-IκBα in 20 mM HEPES pH 7.2, 10 mM $MgCl_2$, 0.35 mM $MnCl_2$, 850 ng BSA, 2 μM ATP, 0.1 μCi 33Pγ ATP and test compound at a suitable concentration were incubated for 60 min at room temperature. The same conditions were used for IKK-1, except 1 μg of GST-IκBα (1–53) was used. The kinase reaction was then stopped by addition of ice-cold 50 μL 20% (v/v) trichloroacetic acid (TCA) containing 200 mM ATP. Proteins were allowed to precipitate for 10 min before filtration through a Packard Unifilter onto Packard GF/C filter 96-well plates. Wells were washed six times with 2% (v/v) TCA and dried at 30–40 °C for 60 min. Radioactivity was counted after the addition of 25 μL Microscint-40 on a Packard topcount microplate scintillation counter.
13. Peripheral blood mononuclear cells (PBMCs) were prepared from human whole blood using LymphoPrep separation, counted using a haemocytometer and diluted to 2.6×10^6/mL in cell medium {RPMI 1640 supplemented with 2 mM glutamine, 1% (v/v) heat inactivated human A–B serum and 100 IU/mL of penicillin and streptomycin}. PBMCs (100 μL) were cultured with test compounds (50 μL) in tissue culture treated 96-well plates 30 min prior to the addition of bacterial endotoxin lipopolysaccharide (LPS) (*E. coli* type 0111:B4: 50 μL of 4 μg/mL) and then incubated for a further ~16 h. The production of TNFα in response to LPS by the PBMCs was stopped by removal of the cell medium from the PBMCs by aspiration. TNFα in the cell assay medium was quantitated using a conventional enzyme-linked immunosorbent assay and nonspecific compound effects on PBMC viability measured by incubation of the remaining treated cells in a WST-1 based cytotoxicity assay.
14. Thiophenecarboxamide **1** has also been identified by others as an IKK-2 inhibitor see Kishore, N.; Sommers, C.; Mathialagan, S.; Guzova, J.; Yao, M.; Hauser, S.; Huynh, K.; Bonar, S.; Mielke, S.; Albee, L.; Weier, R.; Graneto, M.; Hanau, C.; Perry, T.; Tripp, C. S. *J. Biol. Chem.* **2003**, *278*, 32861.
15. Davis, R. V.; Fraser, J. EP209977.
16. Hu, M. C. T.; Wang, Y.-P. *Gene* **1998**, *222*, 31.
17. Lawrie, A. M.; Noble, M. E.; Tunnah, P.; Brown, N. R.; Johnson, L. N.; Endicott, J. A. *Nat. Struct. Biol.* **1997**, *4*, 796.
18. Schulze-Gahmen, U.; De Bondt, H. L.; Kim, S. H. *J. Med. Chem.* **1996**, *39*, 4540.
19. Sicheri, F.; Moarefi, I.; Kuriyan, J. *Nature* **1997**, *385*, 602.
20. Šali, A.; Blundell, T. L. *J. Mol. Biol.* **1993**, *234*, 779.
21. Brooks, B. R.; Bruccoleri, R. E.; Olafson, B. D.; States, D. J.; Swaminathan, S.; Karplus, M. *Comp. Chem.* **1983**, *4*, 187.
22. Connolly, M. L. *Science* **1983**, *221*, 709.
23. Ghose, A. K.; Crippen, G. M. J. *Comp. Chem.* **1986**, *7*, 565.